PROJECT TITLE: Transition of the Coastal and Estuarine Storm Tide Model to an Operational Model
                  for Forecasting Storm Surges
CONTRIBUTORS: Keqi Zhang, Yuepeng Li, and Yi-Cheng Teng
PERFORMANCE PERIOD: 09/01/2015 through 02/29/2016

Percentage of Work Completed: 22%

Project Proceeding on Schedule: [√] Yes   [ ] No

Describe milestones achieved (publications, technology transferred, outreach actions, other results):

1. Background

The coastal and estuarine storm tide (CEST) model developed by Zhang et al (2008; 2012) has a potential to satisfy the National Hurricane Center (NHC)'s operational needs for surge forecasting. CEST overcomes the limitations of Sea, Lake, and Overland Surges from Hurricanes (SLOSH) by solving the full momentum equations that include non-linear advective acceleration, diffusion terms, and bottom friction influenced by the land cover effect.

The depth-averaged 2D CEST model over orthogonal curvilinear grids, which can run on conformal grids such as those used by SLOSH without additional modification of the numerical algorithms, is used to simulate storm surges. Recently, 27 active basin data, including data files for simulation, shape files for Basins (Fig. 1), and synthetic storm track files, were provided to the CEST team by NHC. For each basin, there are a total of 10,000-20,000 synthetic tracks for hypothetical hurricanes with various categories, approaching directions, moving speeds, radiuses of maximum wind, and landfall positions.

One of the requirements to transfer a surge model in a research mode into an operation model is to develop the capability of conducting surge simulations over existing SLOSH basins and reproducing associated MEOW and MOM products. This would allow an operational center such as NHC to potentially adopt a new modeling system without incurring the tremendous costs associated with transitioning, building, and maintaining a new set of model grids. Furthermore, the simulated results must be in a geographic information system format to facilitate the usage of surge flooding data across many platforms by evacuation-planners, decision-makers and the scientific community.

In addition, the CEST model has to conduct simulations using synthetic storms on each basin with computational time comparable to SLOSH for real time forecasting and ensure the stability of CEST by examining modeled results. In order to reduce the computational time for a large set of hypothetical storms, a high performance computing servers with multi-core processors have been used to conduct simulations.
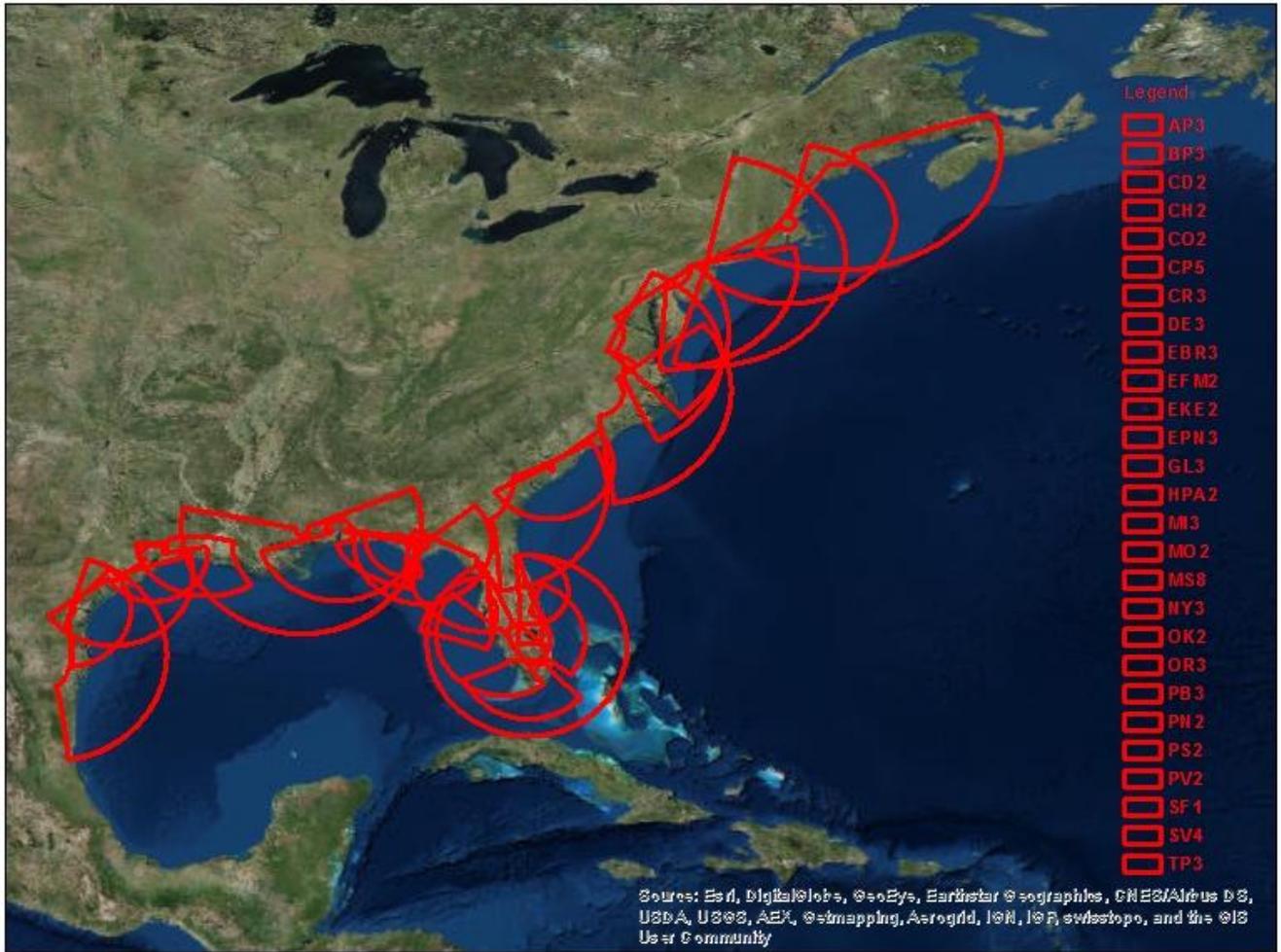
Fig. 1. Active 27 SLOSH basins along the U.S. Atlantic and Gulf Coasts.

2. Objective

According to the timeline of this project, the major tasks during this phase are transferring the updated SLOSH basins into CEST grids:

(1) Converting updated SLOSH grids into CEST grids and running CEST on SLOSH basins using 10,000-20,000 synthetic hurricanes for the basins to ensure the numerical stability;

(2) Generating and comparing MEOW and MOM maps using multiple CEST and SLOSH simulations for the basins;

(3) Testing the computational time on the High Performance Computing (HPC) center of Florida International University (FIU).

3. Converting a SLOSH grid to the CEST grid

The computational scheme of the SLOSH model is based on Arakawa B-grid (Jelesnianski et al. 1992; Purser and Leslie 1988) with velocity components at the four corners of a grid cell and the elevation at the center. By contrast, the computational scheme of the CEST model is based on the modified Arakawa C-grid (Blumberg and Mellor 1987; Purser and Leslie 1988) with velocity components at the four edges of a grid cell and the elevation at the center. The elevations at four edges are also included into the numerical scheme to simulate wetting and drying processes using the accumulative volume method (Zhang et al. 2008). The following procedure has been developed to convert a SLOSH grid and associated subgrid features into the CEST grid (Zhang et al. 2013).

3.1. Grid Coordinate:
Extract the grid coordinates from the SLOSH shapefile and create the grid for CEST.

3.2. Cell Center Depth:
Set the center depth of a CEST cell to be the depth of SLOSH cell center.

3.3. Edge Depth:
Set edge depths of a CEST cell by averaging center depths of two adjacent CEST cells.

3.4. Barrier Depth:
Update the depth of an edge by averaging depths of two adjacent SLOSH barrier points that are connected by the edge.

3.5. Flow Depth:
a. Update the center depths of the cell at the left (D_L) and right (D_R) sides of the edge coincidence with a flow point using a width weighting method:

$$\begin{cases} D_L = w * D_{flow} + (1-w)D_{LO} \\ D_R = w * D_{flow} + (1-w)D_{RO} \end{cases} \quad (1)$$

where w is the ratio of the flow width to the edge width, D_{flow} is the depth of the SLOSH flow point, D_{LO} is the original center depth of the cell at the left side of the edge, and D_{RO} is the original center depth of the cell at the right side of the edge.

b. Update the depth (D_E) of the flow edge using center depths of two adjacent cells

$$D_E = Max(D_L, D_R) \quad (2)$$

3.6. Cut Depth:
Update edge and center depths using the same method for Flow Depth.

3.7. Tree Flag:
Set up the tree flag of a CEST cell based on the value of SLOSH tree point at the top right vertex of the CEST cell. The SLOSH tree values of 2, 5, 6, and 8 are set to be 0 which represents ocean cell in CEST. The SLOSH tree values of 3 and 4 set to be 1 which represents lake cell in CEST. The SLOSH tree value of 1 is set to be 2 to represent the tree cell in CEST. The tree flag is only used for computation of wind field in CEST. The wind speed is adjusted using a coefficient C_T based on the ratio of the surge water depth (D) to the vegetation height (H_T) when the value of tree flag is 2:

$$C_T = \begin{cases} \dfrac{D}{H_T} & D < H_T \\ 1 & D \geq H_T \end{cases} \quad (3)$$

The effect of trees on the wind speed decreases based on this equation as the water submerges the vegetation gradually.

(8) Manning's Coefficients:
Two methods are employed to estimate Manning's coefficients. The first one is based on the following empirical relationship between the water depth (D) in meter and the coefficient (n_a):

$$n_a = \begin{cases} 0.01 + 0.01/D & D > 1 \\ 0.02 & 0 < D \leq 1 \\ 0.02 - 0.01D & -5 < D \leq 0 \\ 0.7 & D \leq -5 \end{cases} \quad \text{or} \quad \begin{cases} n_w & D > 1 \\ n_w & 0 < D \leq 1 \\ 0.02 - 0.01D & -5 < D \leq 0 \\ 0.7 & D \leq -5 \end{cases} \quad (4)$$

where n_w is a constant Manning coefficient for ocean grid cells. The values of n_w range from 0.01 to 0.03, with a typical value of 0.02. It is noteworthy that Manning's coefficients increase as water depths decrease and increase on the land as elevations (negative water depths) increase. This method is applied to the area where the land cover data are not available. When the land cover data are available, the second method is used based on the types of land cover. Manning's coefficient for land grid cells are calculated using,

$$n_a = \frac{\sum_{i=1}^{N}(n_i\alpha) + n_0\beta}{N\alpha + \beta}$$

(5)

where n_i is the Manning's coefficient values of a pixel in the national land cover dataset (NLCD) within a model grid cell, α is the area of a NLCD pixel, N is the total number of NLCD pixels within a model cell, n_0 is a constant Manning's coefficient, 0.02, for the area, β, that are not covered by NLCD pixels. The 2011 NLCD image created by U.S. Geological Survey (Fig.2) are used in Equation 5. Manning's coefficients for ocean grid cells are calculated based on the portion with D>0 in Equation 4.
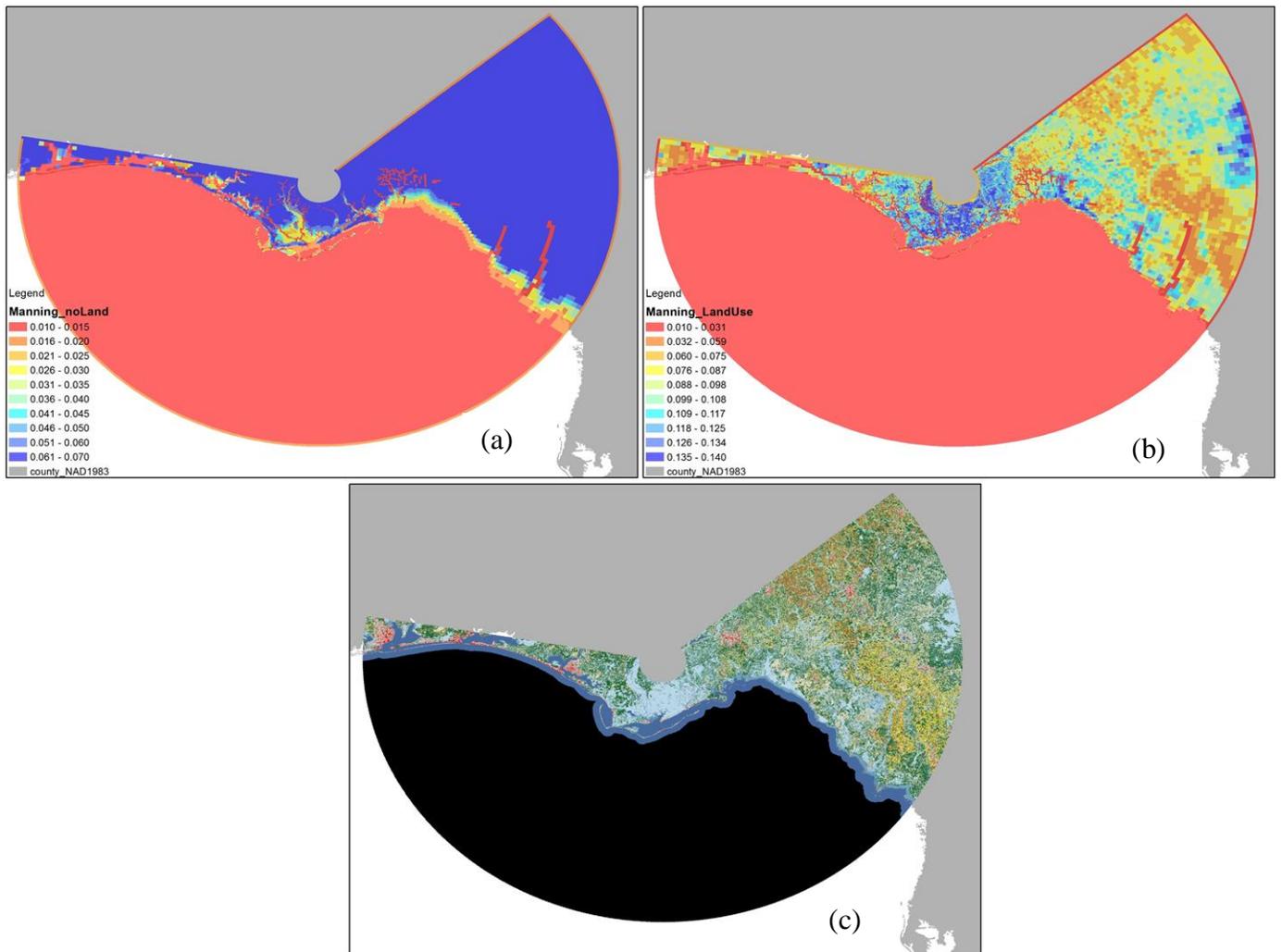

Fig. 2. Manning's coefficient of Apalachicola Bay Basin without incorporating Land Cover Data (a), with considering Land Cover Data (b) and Land Cover Image (c).

4. The spatial pattern comparison of computed MOMs between SLOSH and CEST

At present, 12 SLOSH basins haven been transferred in to CEST grids. These 12 basins are Apalachicola Bay (AP2), Cedar Key (CD2), Cape Canaveral (CO2), Delaware Bay (DE3), Fort Myers (FM2), Galveston Bay (GL3), Florida Bay (KE2), Biscayne Bay (HMI3), Mobile Bay (MO2), New Orleans (MS7), Tampa Bay (TP3), and Norfolk (OR3) basins. Here we selected one basin, Apalachicola Bay (AP3), to present the comparison of computed MOMs and MEOWs by SLOSH and CEST.

The comparison of MOMs between CEST and SLOSH for all categories at mean and high tide are presented at Figs. 3, 4, 5, 6, 7, and 8. The results showed that the overall spatial pattern of maximum storm surges was similar. The maximum surges of each category's MOM showed that CEST produced comparable results to SLOSH (Table 1).

Table 1. Comparison of maximum MOMs generated by CEST and SLOSH at mean and high tide levels in the AP3 basin.

MOMs	SLOSH (mean)	CEST (mean)	SLOSH (high)	CEST (high)
Tropical Storm (ft)	6	5	7	6
Category 1 (ft)	9	8	10	9
Category 2 (ft)	16	16	17	17
Category 3 (ft)	24	24	25	25
Category 4 (ft)	30	29	31	30
Category 5 (ft)	35	35	35	36

However, the inundation area was different in the Apalachicola Bay basin (Table 2). CEST generated less inundation area than SLOSH at all categories (Figs. 3, 4, 5, 6, 7, and 8), even though the maximum surge was similar. One possible reason for this difference was that the friction forces over the land became larger in CEST due to incorporating land cover effects than those in SLOSH which did not consider land cover effects. A larger friction forces caused more resistance to water flow, producing less flooding areas than SLOSH did.

Table 2. Comparison of inundation areas simulated by CEST and SLOSH at the mean and high tide levels in the AP3 basin.

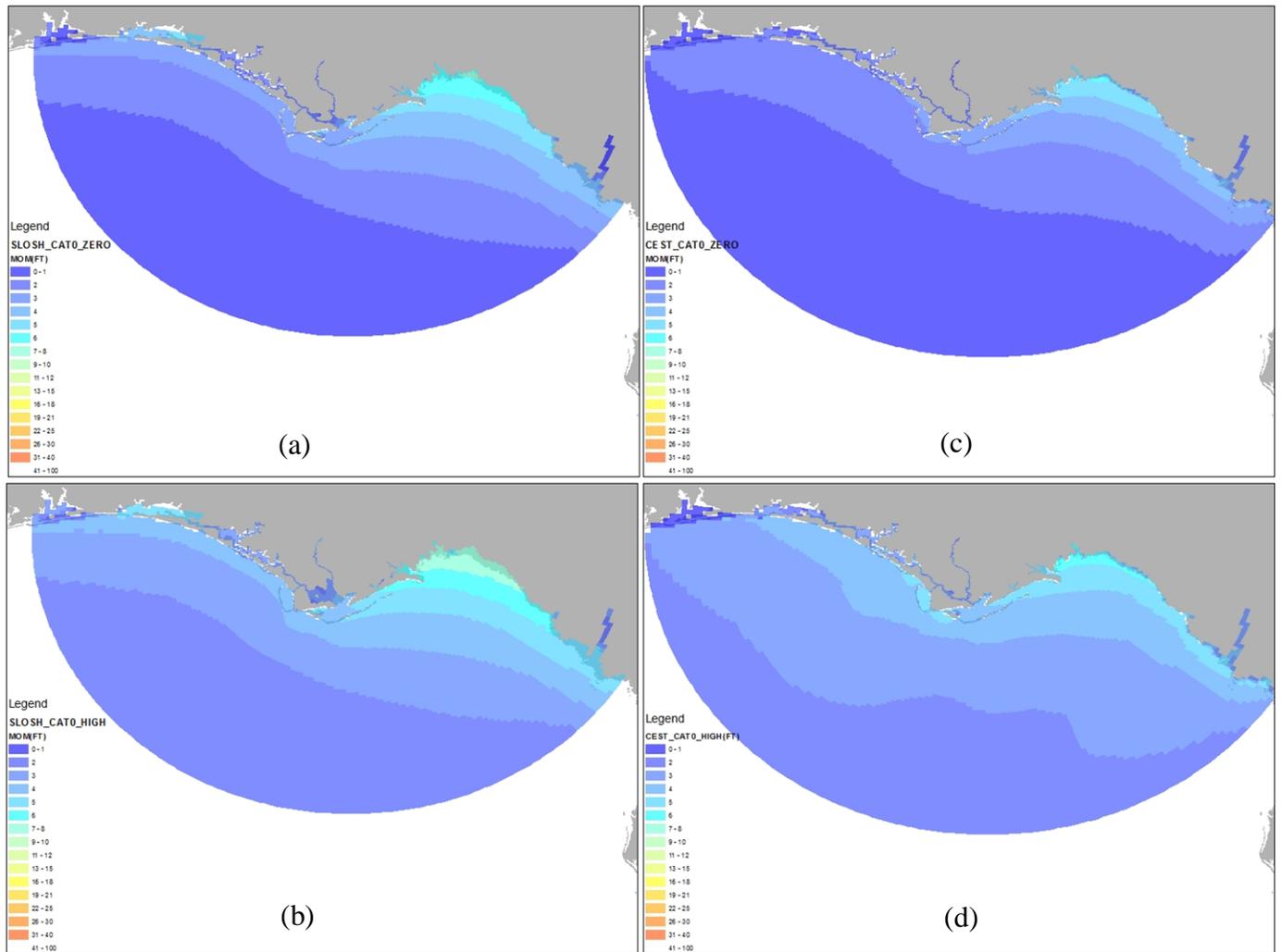| Inundation Area	SLOSH (mean)	CEST (mean)	SLOSH (high)	CEST (high)
Tropical Storm (km^2)	979	423	1387	660
Category 1 (km^2)	1472	742	1785	925
Category 2 (km^2)	2544	1774	2771	1989
Category 3 (km^2)	3911	2641	4210	2776
Category 4 (km^2)	5217	3373	5447	3526
Category 5 (km^2)	6467	4091	6628	4291

Fig. 3. The MOMs of Tropical Storm in the Apalachicola Bay Basin produced by SLOSH at mean tide (a) and at high tide (b), and produced by CEST at mean tide (c) and at high tide (d).
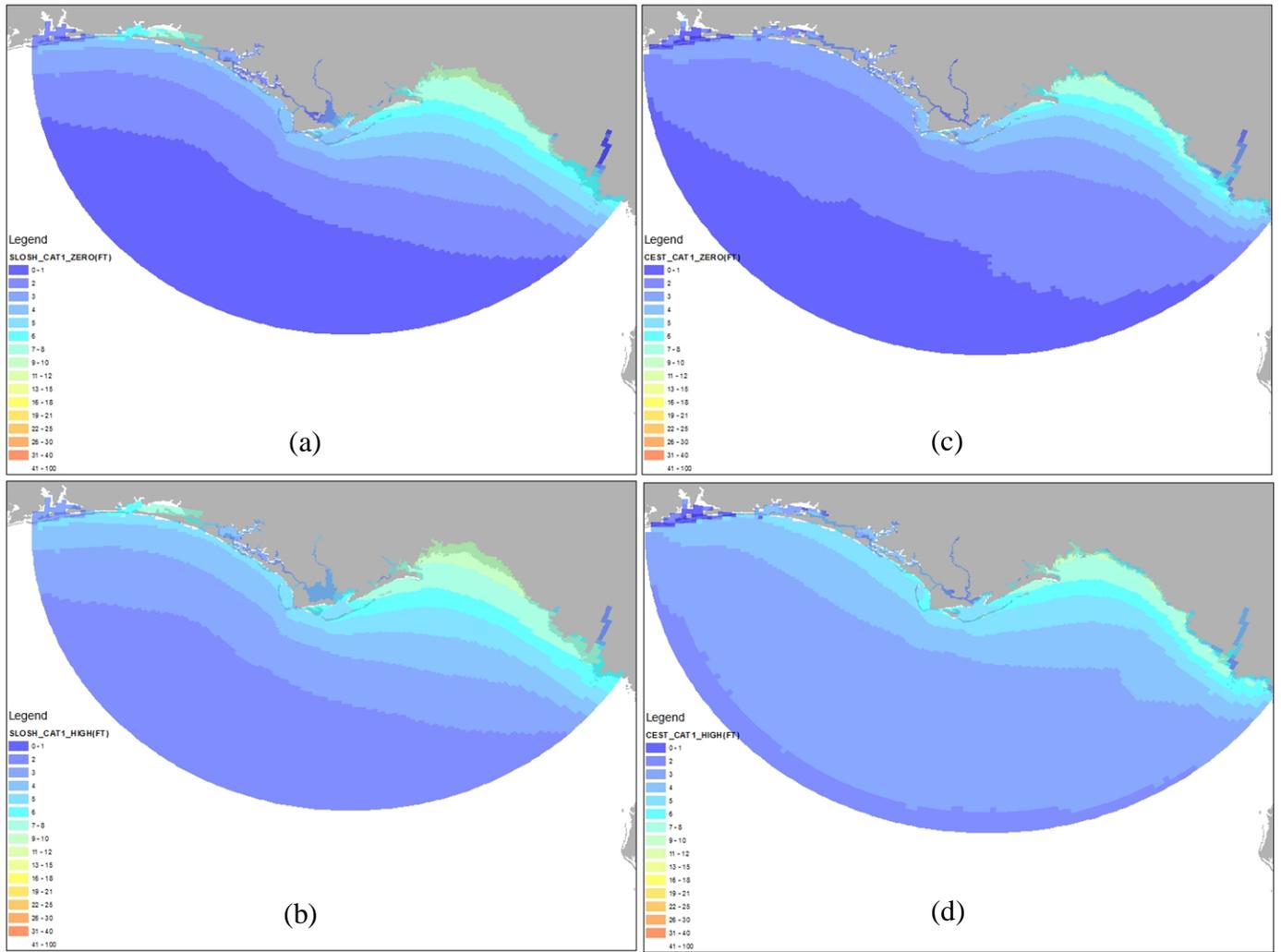
Fig. 4. The MOMs of Category 1 in the Apalachicola Bay Basin produced by SLOSH at mean tide (a) and at high tide (b), and produced by CEST at mean tide (c) and at high tide (d).
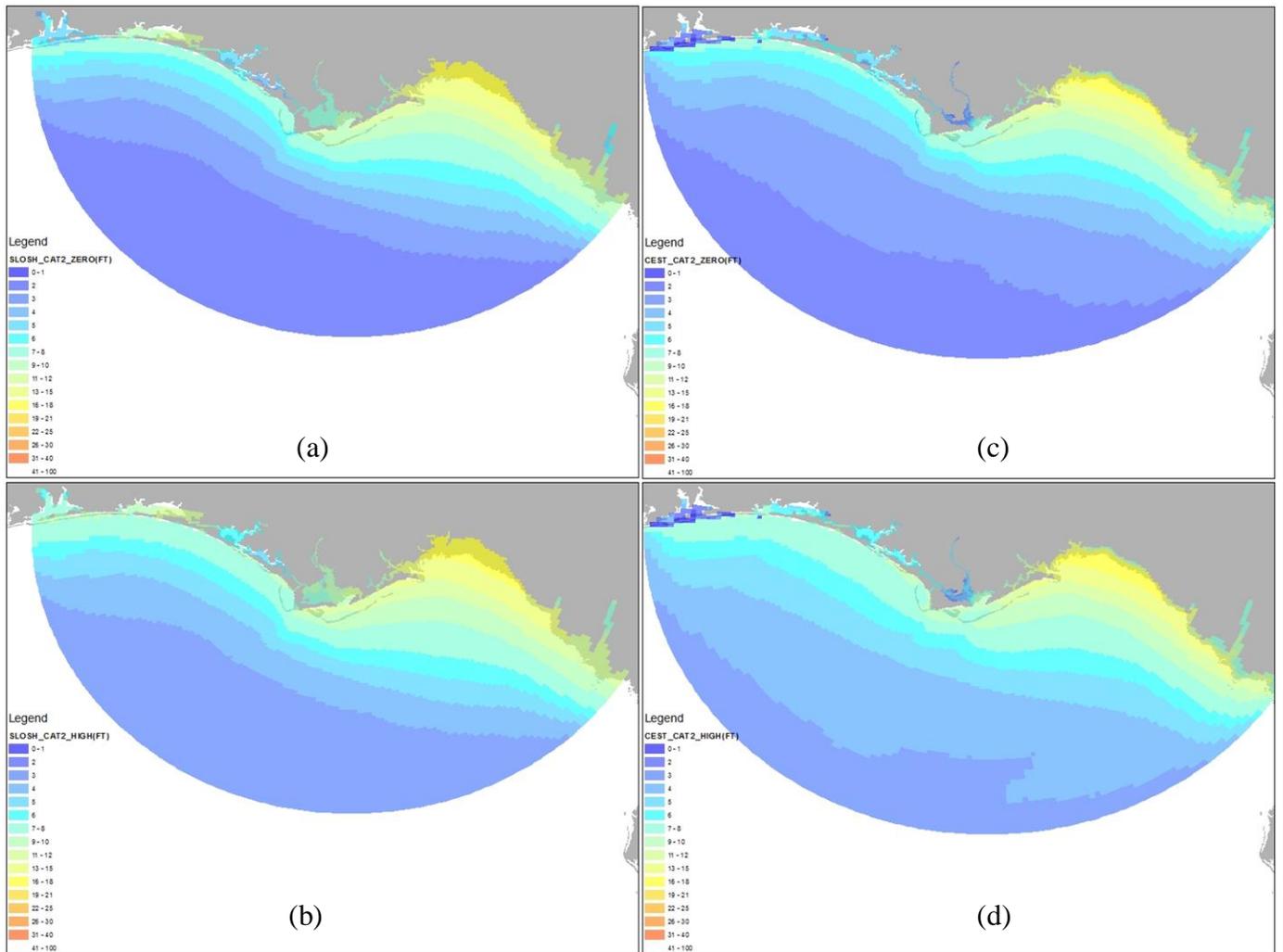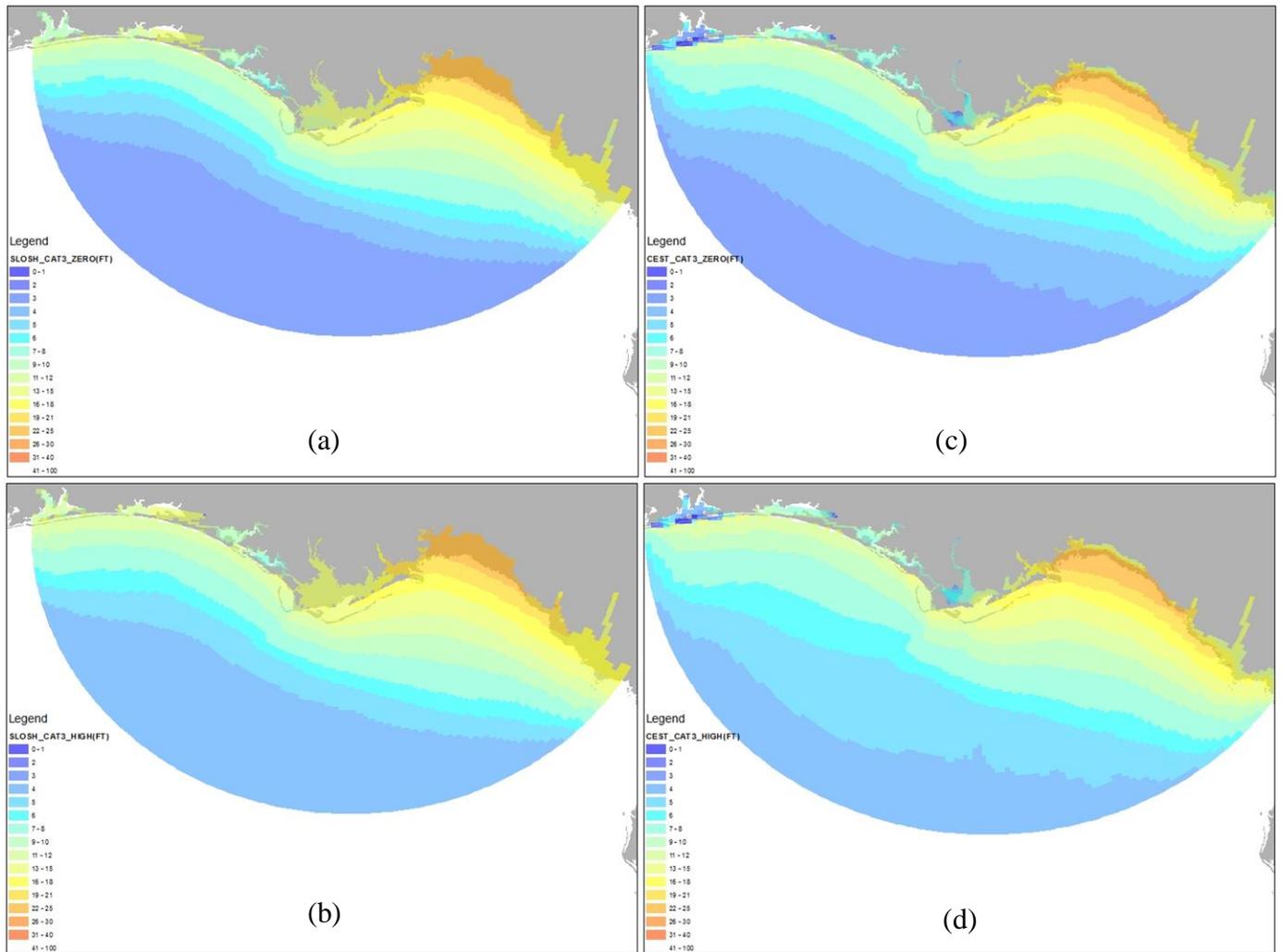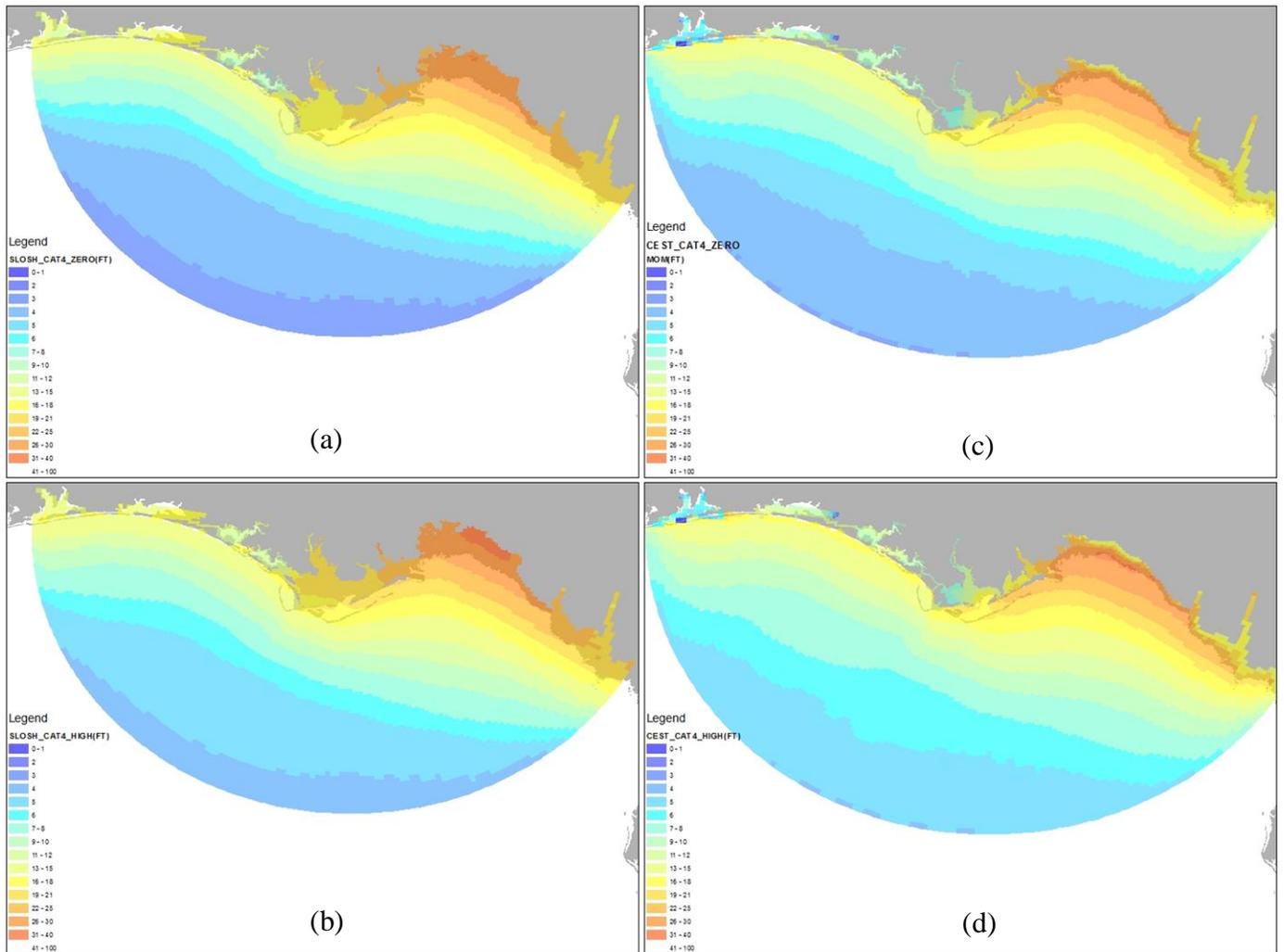
Fig. 5. The MOMs of Category 2 in the Apalachicola Bay Basin produced by SLOSH at mean tide (a) and at high tide (b), and produced by CEST at mean tide (c) and at high tide (d).
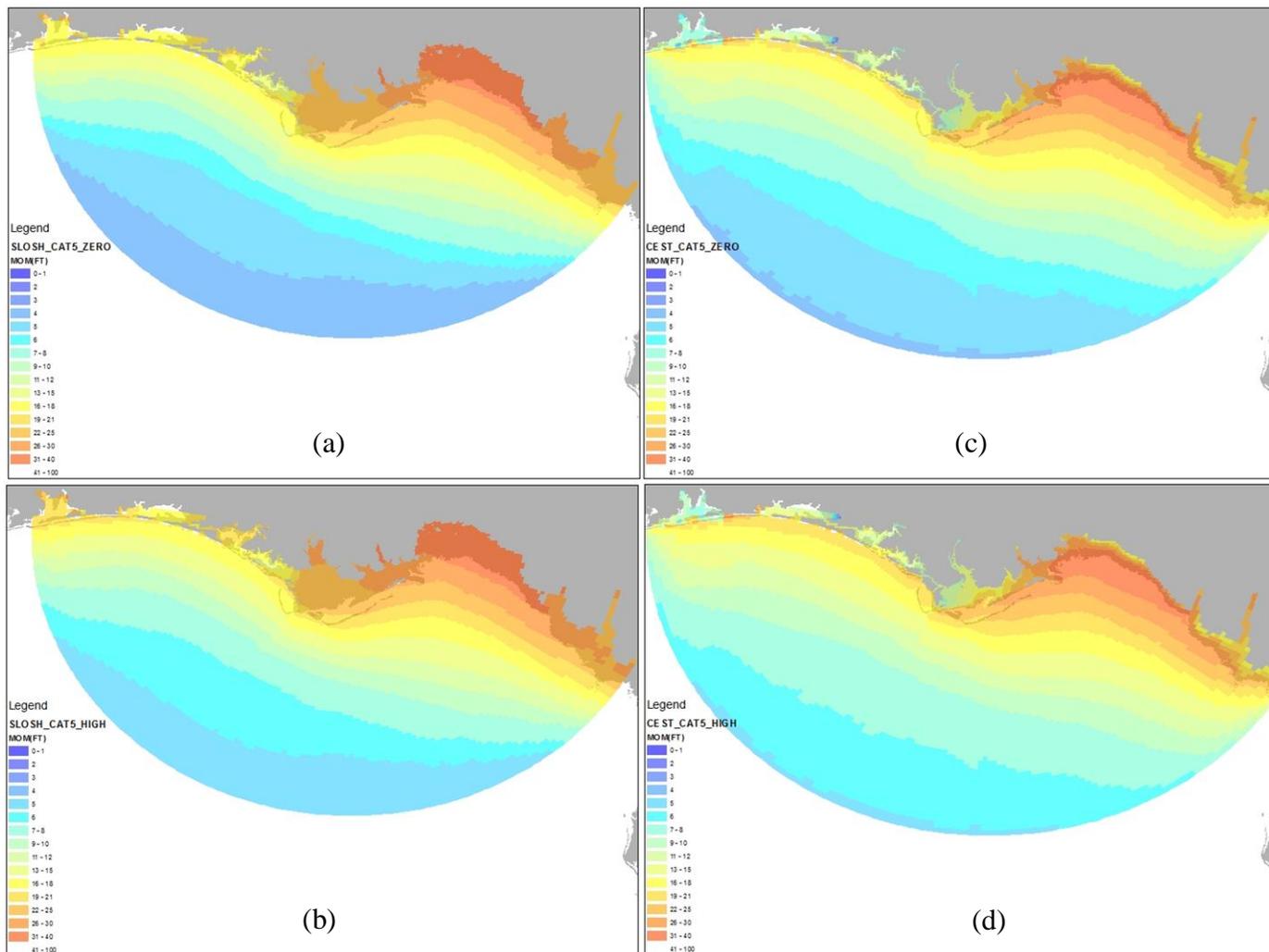
Fig. 6. The MOMs of Category 3 in the Apalachicola Bay Basin produced by SLOSH at mean tide (a) and at high tide (b), and produced by CEST at mean tide (c) and at high tide (d).

Fig. 7. The MOMs of Category 4 in the Apalachicola Bay Basin produced by SLOSH at mean tide (a) and at high tide (b), and produced by CEST at mean tide (c) and at high tide (d).

Fig. 8. The MOMs of Category 5 in the Apalachicola Bay Basin produced by SLOSH at mean tide (a) and at high tide (b), and produced by CEST at mean tide (c) and at high tide (d).

5. The spatial pattern comparison of computed MEOW between SLOSH and CEST

MEOWs were calculated and extracted for the Apalachicola Bay Basin (AP3). The MEOWs at Category 4 and moving speed 5 mph above the mean tide were selected to make the comparison between CEST and SLOSH (Figs. 9, 10, 11, 12, 13, 14, 15, 16, and 17). The maximum surges of each direction's MEOW computed by CEST are comparable with the SLOSH results (Table 3).

Table 3. Comparison of maximum MEOWs (ft) at Category 4 and a moving speed of 5 mph above the mean tide between CEST and SLOSH in the AP3 basin.

MEOWs	SLOSH (mean) ft	CEST (mean) ft
East direct (e)	20	21
East-North-East direct (i)	21	22
North direct (n)	26	25
North-East direct (b)	21	23
North-North-East direct (c)	24	24
North-North-West (f)	26	25
North-West direct (a)	25	24
West direct (w)	20	22
West-North-East (d)	24	24

It appeared that the MEOWs by CEST were comparable to MEOWs by SLOSH as in the cases of MOMs, but with less inundation area from CEST. We are studying the reason for this difference by conducting numerical experiments and analyzing individual simulations from SLOSH and CEST in the next stage.
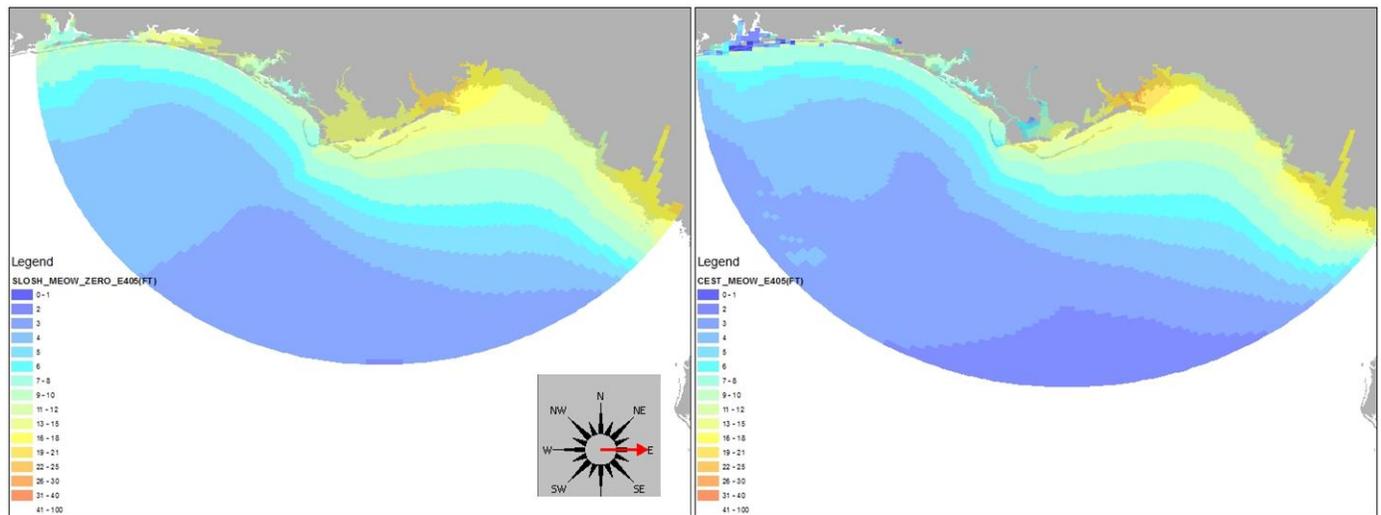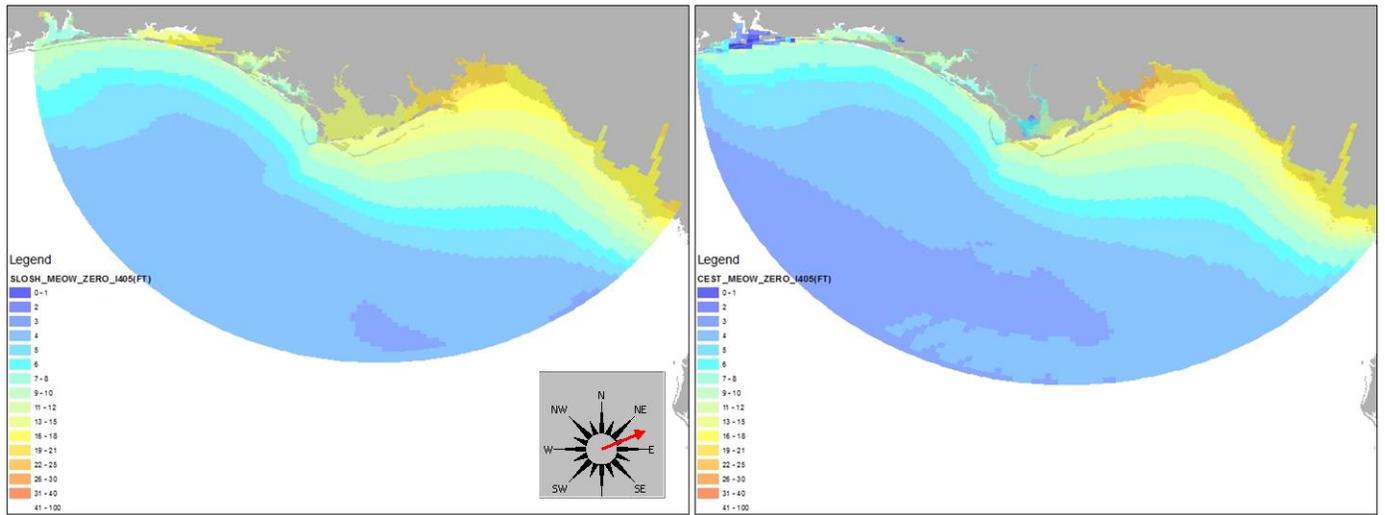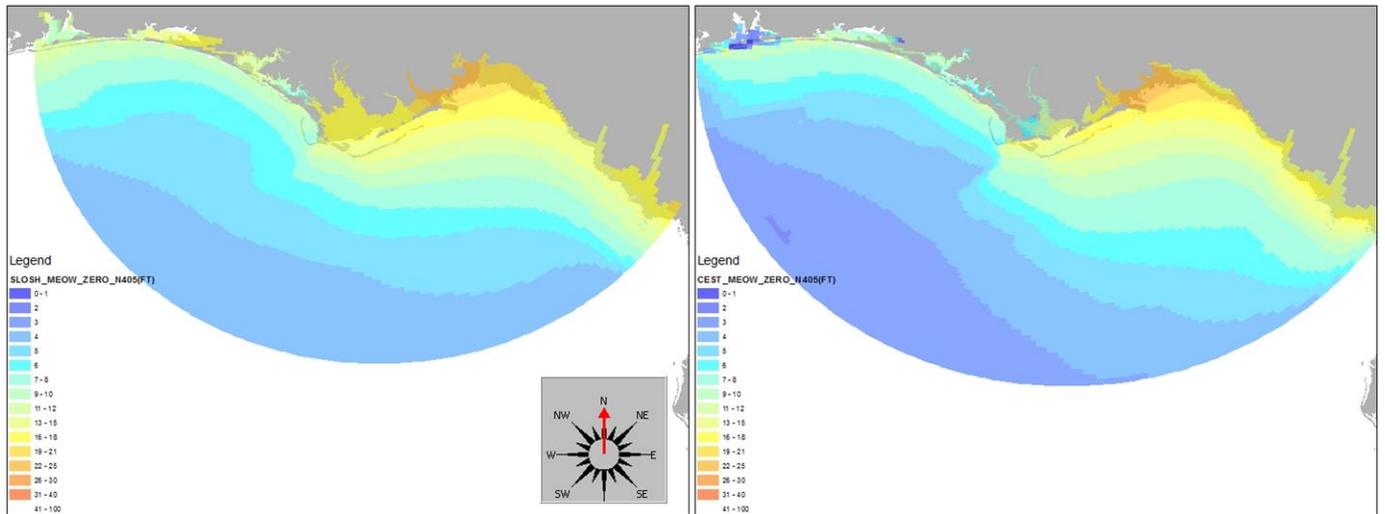

(a)   (b)

Fig. 9. The MEOWs of e405 at mean tide (Direction=East, Category=4, Moving speed=5 mph) in the Apalachicola Bay Basin produced by SLOSH (a) and produced by CEST (b).
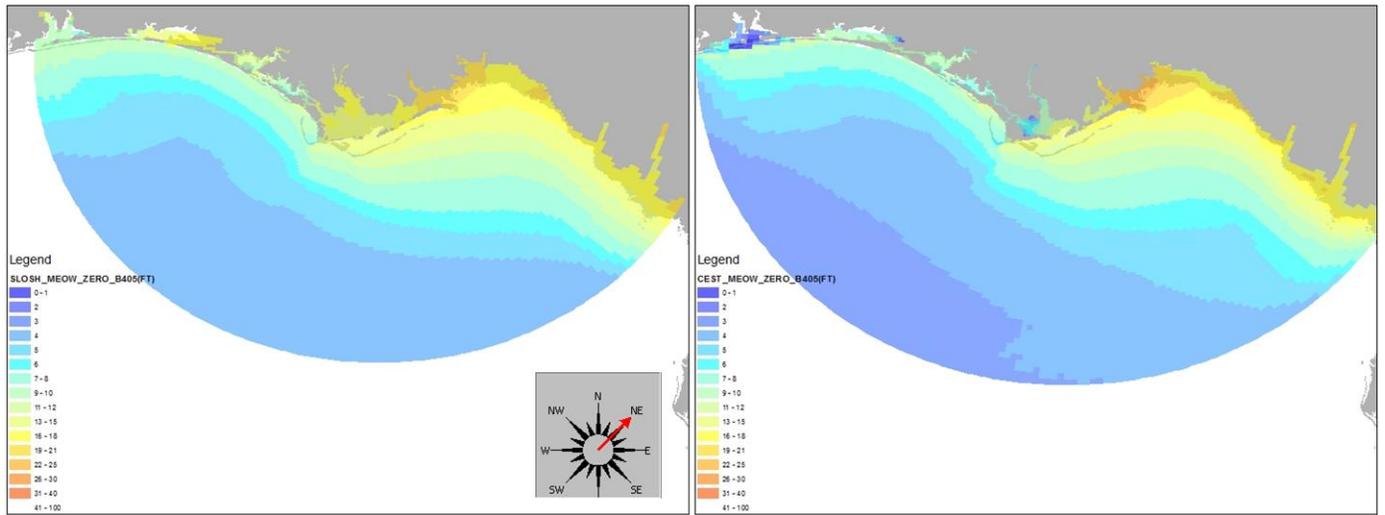
Fig. 10. The MEOWs of i405 at mean tide (Direction=East-North-East, Category=4, Moving speed=5 mph) in the Apalachicola Bay Basin produced by SLOSH (a) and produced by CEST (b).
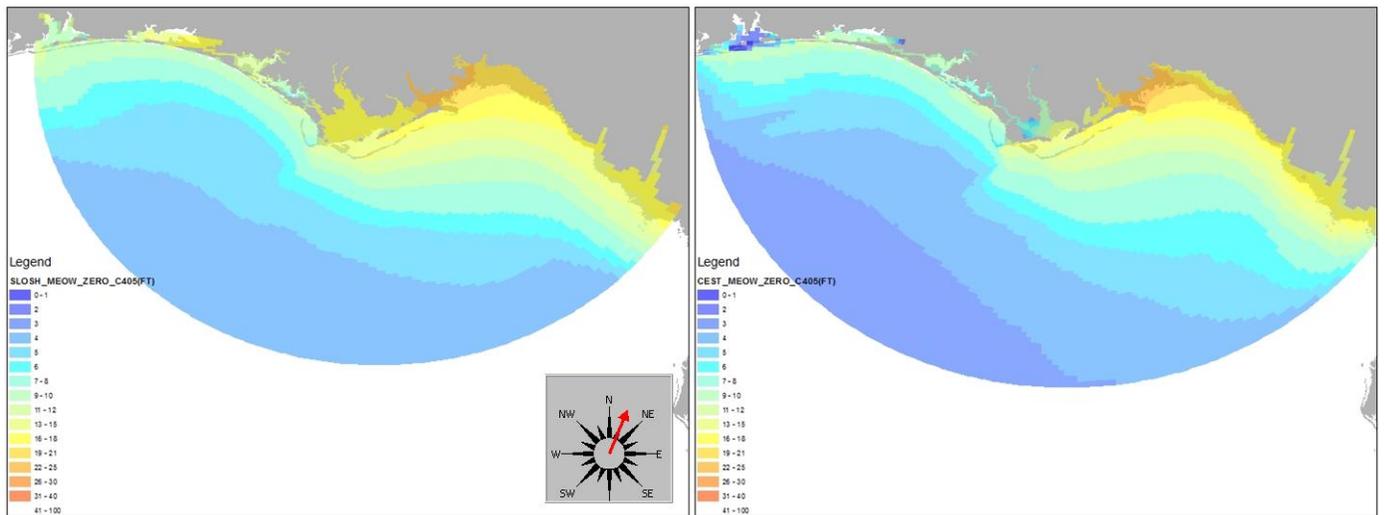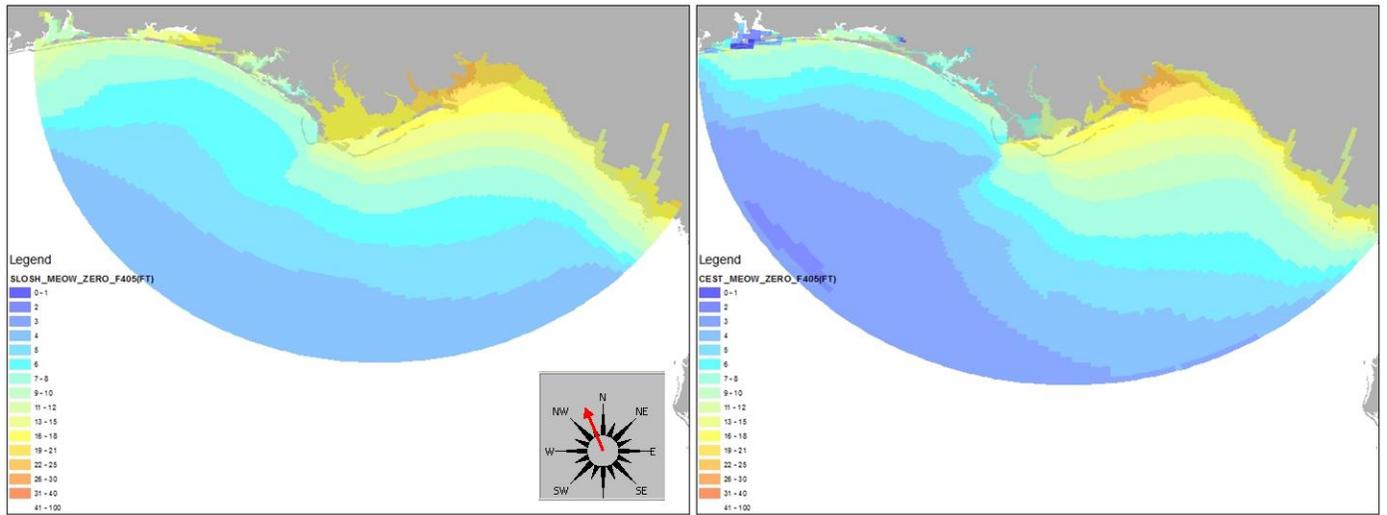

Fig. 11. The MEOWs of n405 at mean tide (Direction= North, Category=4, Moving speed=5 mph) in the Apalachicola Bay Basin produced by SLOSH (a) and produced by CEST (b).
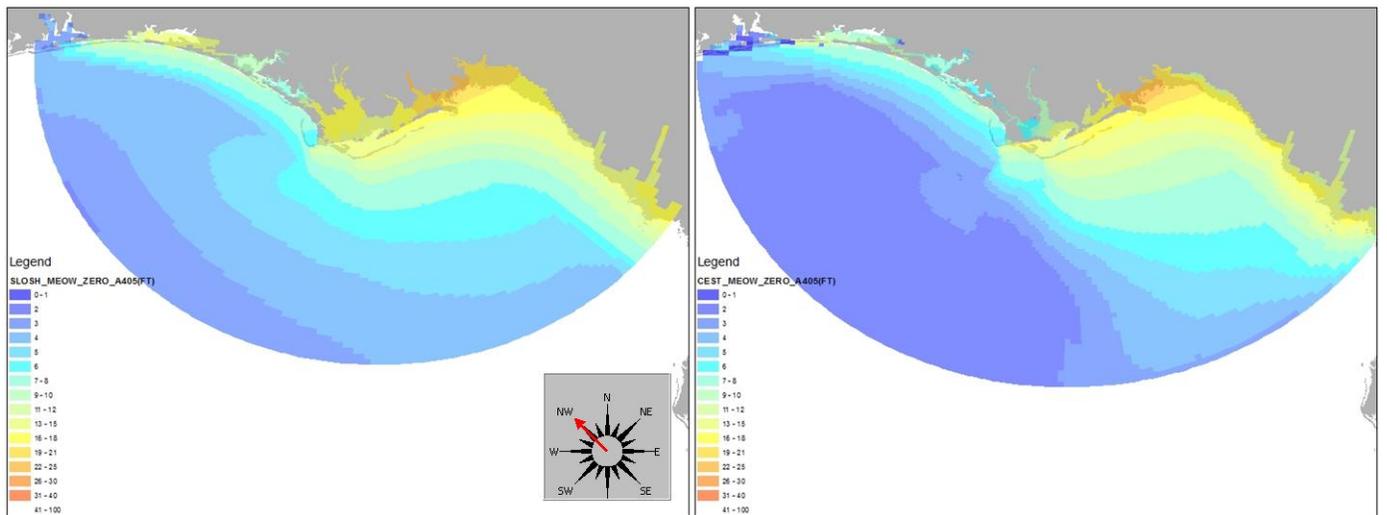
(a)   (b)

Fig. 12. The MEOWs of b405 at mean tide (Direction= North-East, Category=4, Moving speed=5 mph) in the Apalachicola Bay Basin produced by SLOSH (a) and produced by CEST (b).

(a)   (b)

Fig. 13. The MEOWs of c405 at mean tide (Direction= North-North-East, Category=4, Moving speed=5 mph) in the Apalachicola Bay Basin produced by SLOSH (a) and produced by CEST (b).

(a)   (b)

Fig. 14. The MEOWs of f405 at mean tide (Direction= North-North-West, Category=4, Moving speed=5 mph) in the Apalachicola Bay Basin produced by SLOSH (a) and produced by CEST (b).

(a)   (b)

Fig. 15. The MEOWs of a405 at mean tide (Direction= North-West, Category=4, Moving speed=5 mph) in the Apalachicola Bay Basin produced by SLOSH (a) and produced by CEST (b).
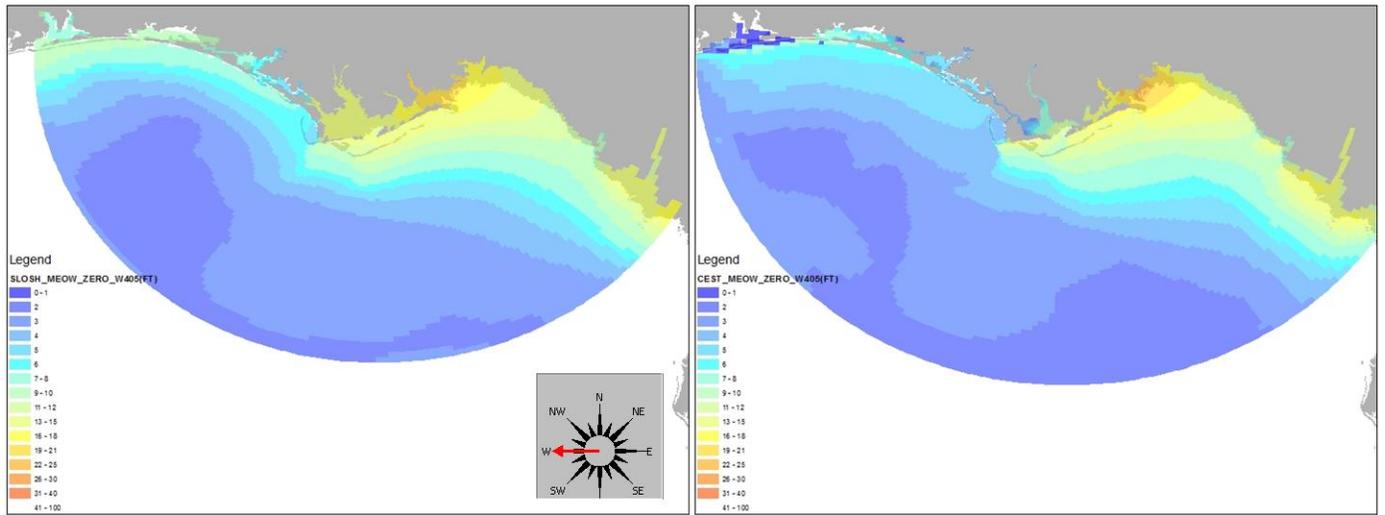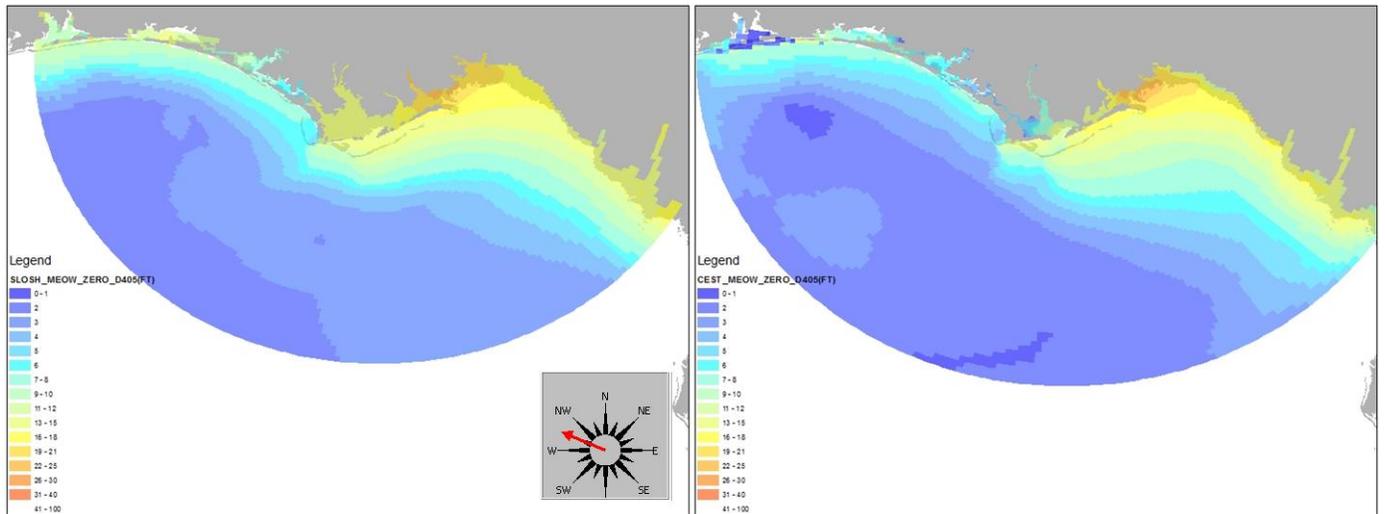
(a)   (b)

Fig. 16. The MEOWs of w405 at mean tide (Direction= West, Category=4, Moving speed=5 mph) in the Apalachicola Bay Basin produced by SLOSH (a) and produced by CEST (b).

(a)   (b)

Fig. 17. The MEOWs of d405 at mean tide (Direction= West-North-West, Category=4, Moving speed=5 mph) in the Apalachicola Bay Basin produced by SLOSH (a) and produced by CEST (b).

6. Computational time on HPC

There are a total of 14,456 synthetic tracks for AP3 basins, and computational time used by the HPC at FIU is about 14 hours with totally 16 cores were used. The average runtime for each core per each case was less than one minute, which is computationally efficient. Therefore, the CEST model has the potential to complete the large ensemble runs within a reasonable time frame if the NOAA's supercomputer with more cores are used.

7. Interaction between National Hurricane Center and Meteorological Development Laboratory

The FIU research team met with the National Hurricane Center team 4 times during the reporting period to discuss the project and exchange the files and documents. The FIU team also had 3 internet video conference calls to discuss the project with staff members of the Meteorological Development Laboratory.

Provide a schedule for the remainder of work to project completion:
- Continuing to convert all SLOSH basins into CEST grid;
- Replicating current operational capabilities (i.e. creation of MOMs, MEOWS, and ensemble runs);
- Discovering the different inundation patterns of MOMs and MEOWs produced by CEST and SLOSH;
- Discovering and developing a prototype of CEST P-Surge.

Describe problems or circumstances affecting completion date, milestones, scope of work, and cost:

Additional Comments/Elaboration:

References:

Blumberg, A. F., and G. L. Mellor, 1987: A description of three-dimensional coastal ocean circulation model. *Three-Dimensional Coastal Ocean Models*, N. S. Heaps, Ed., American Geophysical Union, 1-16.

Jelesnianski, C. P., J. Chen, and W. A. Shaffer, 1992: SLOSH: Sea, lake and overland surges from hurricanes. Technical Report NWS 48, 71 pp.

Purser, R. J., and L. M. Leslie, 1988: A semi-implicit, semi-Lagrangian finite difference scheme using high-order spatial differencing on a nonstaggered grid. *Monthly Weather Review*, **116,** 2069-2080.

Zhang, K., C. Xiao, and J. Shen, 2008: Comparison of the CEST and SLOSH models for storm surge flooding. *Journal of Coastal Research*, **24,** 489-499.

Zhang, K., H. Liu, Y. Li, H. Xu, J. Shen, J. Rhome, and T. J. Smith III, 2012: The role of mangroves in attenuating storm surges. *Estuarine, Coastal, and Shelf Science*, **102-103,** 11-23.

Zhang, K., Y. Li, H. Liu, J. Rhome, and C. Forbes, 2013: Transition of the Coastal and Estuarine Storm Tide Model into an operational storm surge forecast model: A case study of the Florida Coast. *Weather and Forecasting*, **28,** 1019-1037.